Architecture Effects in Complex Spherical Assemblies of $(AB)_n$-type Block Copolymers

Stephanie M. Barbon,[†,#] Jung-Ah Song,[†,#] Duyu Chen,[†] Cheng Zhang,[†,⊢], Joshua Lequieu,[†] Kris T. Delaney,[†] Athina Anastasaki,[†] Manon Rolland,[†] Glenn H. Fredrickson,[‡,§] Morgan W. Bates,*[,†] Craig J. Hawker,*[,†,‡] and Christopher M. Bates*[,†,‡,§]

[†]*Materials Research Laboratory,* [‡]*Materials Department, and* [§]*Department of Chemical Engineering, University of California, Santa Barbara, California 93106, United States*

[⊢]*Australian Institute for Bioengineering and Nanotechnology and ARC Centre of Excellence in Convergent Bio-Nano Science and Technology, University of Queensland, Brisbane, Queensland 4072, Australia*

ABSTRACT

Molecular architecture plays a key role in the self-assembly of block copolymers, but few studies have systematically examined the influence of chain connectivity on tetrahedrally close-packed (TCP) sphere phases. Here, we report a versatile material platform comprising two blocks with substantial conformational asymmetry, A = poly(trifluoroethyl acrylate) and B = poly(dodecyl acrylate), and use it to compare the phase behavior of AB diblocks, ABA triblocks, and $(AB)_3$ and $(AB)_4$ radial star copolymers. Each architecture forms TCP sphere phases at minority A-block compositions ($f_A < 0.5$), namely σ and A15, but with differences in the location of order–order phase boundaries that are not anticipated by mean-field self-consistent field theory simulations. These results expand the palette of polymer architectures that readily self-assemble into complex TCP structures and suggest important design factors when targeting specific phases of interest.

The self-assembly of organic molecules creates a rich array of hierarchical order that influences the properties of soft matter,[1-4] a topic which continues to stimulate research across diverse fields including medicine,[5] electronics,[6-9] and separations.[10] Among the litany of possible materials, block copolymers are particularly popular because key design parameters can be predicted by theory and carefully controlled during synthesis.[11] Historically, in developing a thorough understanding of equilibrium block copolymer phase behavior, significant attention has focused on linear AB diblocks — the simplest possible architecture — culminating in a well-known set of classical mesophases: body-centered cubic (BCC) spheres, hexagonally-packed cylinders (HEX), the double gyroid network (GYR), and lamellae (LAM).[12] (A limited number of other morphologies have been observed in the melt but only occupy a small sliver of phase space, for example, close-packed spheres (CPS)[13] and the O^{70} network.[14-15]) The prototypical phase behavior of AB diblocks shares remarkable similarities with that of more complex architectures also involving two types of building blocks (A and B):[16-17] ABA triblocks,[18-19] alternating multiblocks (ABABA…),[20-21] and radial $(AB)_n$ stars[22-25] form the same morphologies at comparable volume fractions (f_A), as do B-*g*-A combs[26-27] and A_mB_n miktoarm stars[28-29] but withorder–order phase boundary deflection as a consequence of architectural asymmetry.

Recent discoveries surrounding the phase behavior of linear AB diblock copolymers have significantly altered this classical picture of self-assembly. Two new equilibrium morphologies — σ[30] and A15[31] — have been identified that belong to a class of structures known as topologically close-packed (TCP) phases,[32-33] in addition to several related, kinetically-accessible variants including C14, C15,[34] and an aperiodic dodecagonal quasicrystal.[35] These exotic unit cells, which are also found in inorganic alloys[36] and liquid crystals,[37-39] share a common packing motif constructed from irregular, tetrahedral groupings of micelles arranged in characteristic Frank–

Kasper coordination polyhedra.[40] The formation of soft TCP phases in block copolymers has been theoretically predicted by Shi,[41-42] Grason,[28, 43-45] and coworkers to arise from conformational asymmetry, a measure of the distinct space-filling tendency of each block.[46] There are two strategies for achieving large values of conformational asymmetry through molecular design as parameterized by $\varepsilon = (b_A/b_B)(n_B/n_A)$ — increase the ratio of block statistical segment lengths (b_A/b_B) and/or introduce arm-number asymmetry (n_B/n_A), i.e., mikto junctions.[47] (Recent simulations have explored even more complicated branched architectures that require additional parameters to fully account for similar conformational effects.[48]) Large values of conformational asymmetry ($\varepsilon \gg 1$) stabilize mesophase geometries with greater interfacial curvature to higher values of f_A.[49-50] Equilibrium TCP phases emerge if there is sufficient conformational asymmetry to stabilize spheres in the vicinity of compositions that would otherwise form HEX in conformationally symmetric analogues ($\varepsilon \approx 1$).[51]

Given the similarities in the classical self-assembly of all AB-type block copolymers, one might expect to find TCP phases with any architecture involving two types of blocks (A and B) and substantial conformational asymmetry ($\varepsilon \gg 1$). Current theory and experiments only hint at this possibility. To the best of our knowledge, the only conformationally-asymmetric AB-type block copolymers beyond linear AB diblocks that have been analyzed in this context by both theory and experiments are AB_n miktoarm stars (n = 2–5). Grason[28] and Xie[41] carried out self-consistent field theory (SCFT) simulations that indicate AB_n miktoarm stars should stabilize the A15 and σ phases, which was recently verified by scattering experiments.[52-53]

Here, we compare the melt phase behavior of AB, ABA, $(AB)_3$, and $(AB)_4$ linear and star block copolymers with A = poly(trifluoroethyl acrylate) and B = poly(dodecyl acrylate) to yield insights into the self-assembly of conformationally asymmetric and highly segregated samples of

varying architecture. The discovery of σ and A15 in ABA, $(AB)_3$, and $(AB)_4$ materials qualitatively mirrors the phase behavior of AB control samples but with differences in order–order phase boundaries that are not accounted for by SCFT simulations. In summary, our results show the formation of TCP phases is a general phenomenon shared by all AB-type block copolymers with the appropriate choice of A and B block chemistry.

In designing a material platform to study the phase behavior of homologous AB-type block copolymers, we sought a pair of A and B monomers that (1) polymerize via the same mechanism to facilitate sequential block growth, (2) have significantly different statistical segment lengths to accentuate conformational asymmetry, (3) exhibit a relatively large interaction parameter (χ) that promotes microphase separation at the low degrees of polymerization (N) known to favor TCP phase formation,[54] and (4) have low-temperature glass and melting transitions (e.g., T_g and T_m < 25 °C) that facilitate processing and annealing. To satisfy these design criteria, we were drawn to two acrylate derivatives: trifluoroethyl acrylate and dodecyl acrylate which can be polymerized via photo-mediated atom transfer radical polymerization (ATRP) — a versatile technique that produces polymers with low molar mass dispersities and high chain-end fidelity (Figure 1).[55-57]

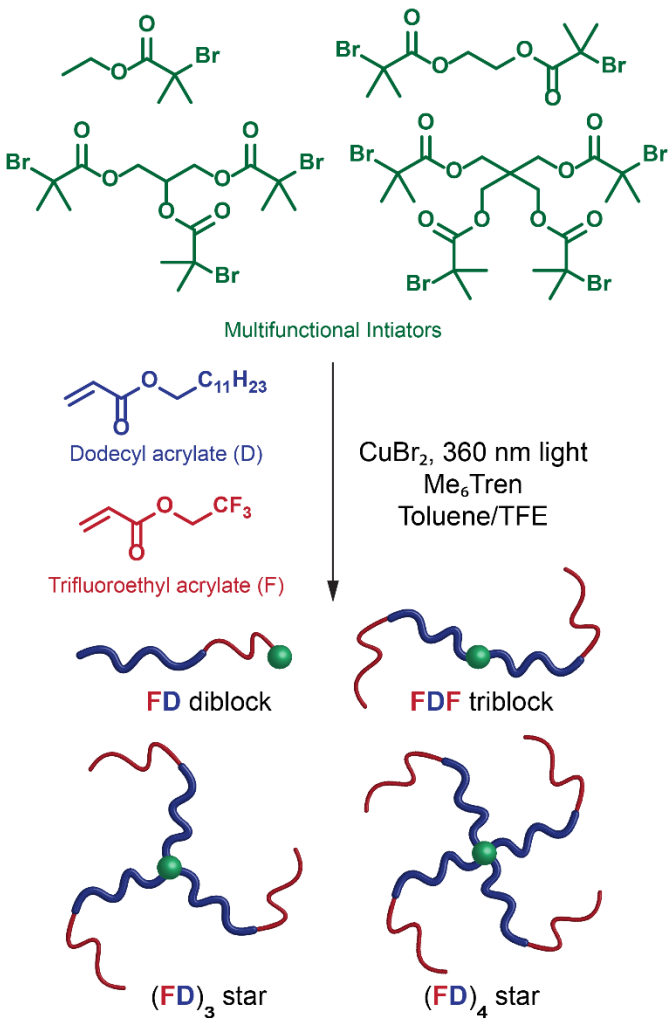

Figure 1. Block copolymer architectures studied in this work with A = poly(trifluoroethyl acrylate) (F, red) and B = poly(dodecyl acrylate) (D, blue) blocks synthesized via sequential photo-mediated ATRP. Below, these materials are studied at minority compositions of the F block ($f_F \leq 0.5$), which forms the core of spherical domains.

We hypothesized that poly(trifluoroethyl acrylate) (F) and poly(dodecyl acrylate) (D) blocks would have significantly different statistical segment lengths resulting in conformational asymmetry that stabilizes TCP phases at minority compositions of the F block ($f_F \leq 0.5$). This assumption is predicated on a trend known in the literature that qualitatively relates the statistical segment length to monomer structure.[46, 58] In general, for a given polymer backbone, increasing

the size of the monomer pendant group decreases b. The substantial difference in size of $–CH_2CF_3$ (F) versus $–C_{12}H_{25}$ (D) should therefore enhance conformational asymmetry by reducing the statistical segment length of the D block ($b_F > b_D$). To estimate the magnitude of this effect, high molecular weight (≥120 kg/mol) poly(dodecyl acrylate) (D) and poly(trifluoroethyl acrylate) (F) homopolymers were synthesized by photo-mediated ATRP, which proceeds under UV irradiation in the presence of an aliphatic tertiary amine ligand (Me_6-Tren) and low concentrations of $CuBr_2$ (Table S1). The measurement of F and D entanglement molecular weights by oscillatory rheology (Figure S8) yielded an estimate of $\varepsilon = b_F/b_D$ = (5.0 Å)/(3.5 Å) = 1.43 at 25 °C with a reference volume v_0 = 118 Å^3 using universal correlations identified by Fetters (see Supporting Information).[59-60] We note that this value of b_D as measured by rheology is somewhat different than previous estimates based on neutron scattering (b_D = 4.3 Å at 25 °C with v_0 = 118 Å^3);[31] due to the absence of any literature reporting b_F from neutron scattering, here we use rheology-derived values of b_D for internal consistency. As a point of comparison, the σ phase forms in poly(isoprene-*block*-lactide)[51] with $\varepsilon \approx 1.15$, and both σ and A15 emerge in poly(lactide-*block*-dodecyl acrylate)[31] with $\varepsilon \approx 1.85$. Our estimated conformational asymmetry ($\varepsilon \approx 1.43$) is therefore likely high enough to stabilize these morphologies.

The presence of fluorine in one block also gives rise to a large interaction parameter (χ) that promotes the formation of TCP phases by facilitating self-assembly at low degrees of polymerization (N);[54] note for all architectures we define N as the length of one diblock arm, so the total degree of polymerization of FD, FDF, $(FD)_3$, and $(FD)_4$ is N, $2N$, $3N$, and $4N$, respectively. To measure χ, we prepared a series of near-symmetric ($f_F \approx 0.50$) poly(trifluoroethyl acrylate-*block*-dodecyl acrylate-*block*-trifluoroethyl acrylate) triblock samples (denoted FDF) with varying N using photo-mediated ATRP and the difunctional initiator ethylene bis(2-bromoisobutyrate)

(Figure 1). These telechelic macroinitiators were chain extended with trifluoroethyl acrylate to yield FDF triblock copolymers with controlled molecular weights and narrow molar mass dispersities $Đ$ (Table S3, Figure S9). To prevent bimolecular coupling, the second F-block polymerizations were terminated at approximately 60% conversion. After measuring order–disorder transition temperatures (T_{ODT}s) of the FDF triblocks by oscillatory rheology using isochronal temperature ramps, χ was estimated by applying the mean-field approximation $(\chi 2N)_{ODT} = 17.996$ (Figure S10). The resulting expression, $\chi(T) = 84/T - 0.101$, was assumed to be identical for all architectures.[18] Finally, both the D and F homopolymers have a T_g below room temperature (Table S1) and the predominant thermal transition measured in FD copolymers is the melting of D-block crystals circa 0 °C (Figure S12). These materials are therefore readily processible at elevated temperatures ($T \geq 25$ °C).

In a similar manner to the compositionally-symmetric FDF triblocks described above, we synthesized a library of FD, FDF, $(FD)_3$, and $(FD)_4$ samples across a wide range of F-block volume fractions ($f_F \approx 0.15 - 0.50$) by sequential photo-mediated ATRP using the initiators illustrated in Figure 1. This diversity allows the dependence of phase behavior on molecular architecture to be studied in detail. All samples were synthesized with only minor modifications of the solvent composition and targeted conversion to prevent bimolecular coupling. Figure 2 shows representative size exclusion chromatograms (SECs) of FD, FDF, $(FD)_3$, and $(FD)_4$ samples with low molar mass dispersities ($Đ \leq 1.08$); see the Supporting Information for full characterization (Tables S2–S5).

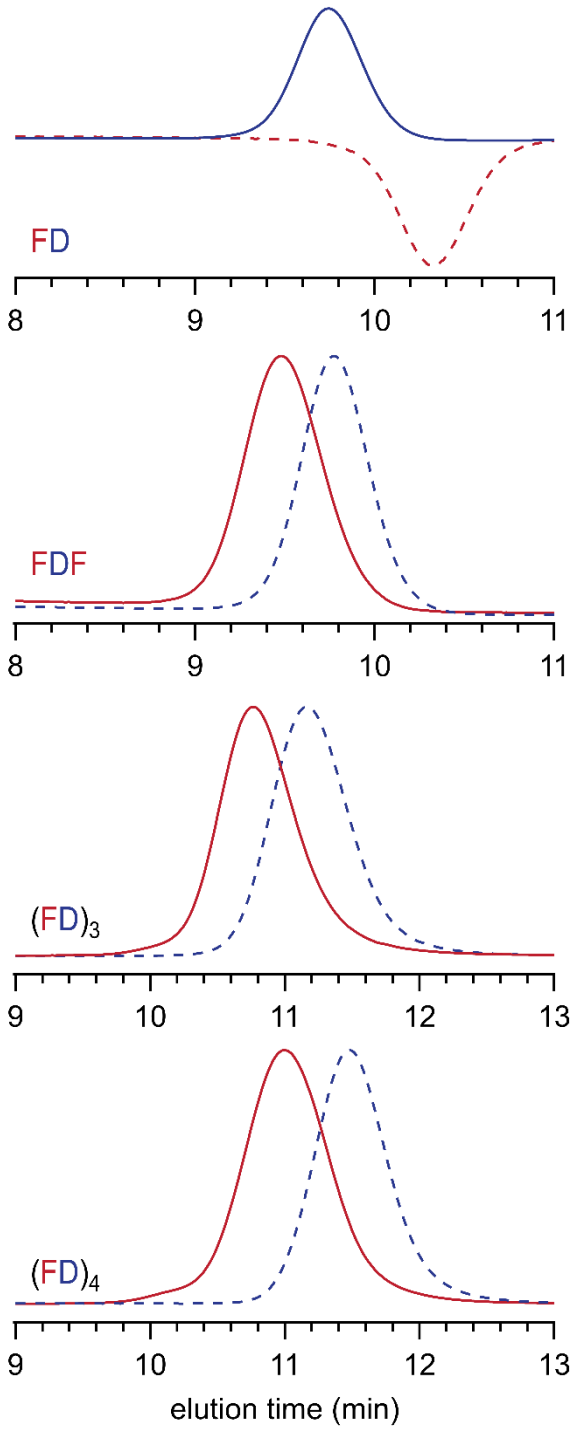

Figure 2. SECs (normalized differential refractive index signal) of FD, FDF, $(FD)_3$, and $(FD)_4$ samples synthesized by photo-mediated ATRP. Note that with the FD diblock, F was polymerized first (dashed red line) followed by D (blue solid curve). In the other three architectures, D was polymerized first (dashed blue line) followed by F (solid red line). In all cases, $Đ \leq 1.08$.

All four architectures self-assemble into high quality TCP phases with aggregation of the shorter F blocks forming the interior of each micelle. Figure 3a,b highlights the discovery of σ and A15 at compositions circa $f_F \approx 0.25$ and 0.30, respectively, in FD, FDF, and $(FD)_4$ as demonstrated by synchrotron small angle X-ray scattering (SAXS). In each sample of Figure 3a,b, morphologies with long range order are evident from the sharp and numerous Bragg reflections that closely match the expected Miller indices of σ ($P4_2/mnm$) and A15 ($Pm\bar{3}n$) space groups (for pattern indexing, see Figures S20–21).[61] $(FD)_3$ also forms A15 (see Figure S14), however, the lower compositional resolution of our $(FD)_3$ library misses an interval ($f_F = 0.22$–0.27) that likely contains the σ phase (Table S4). Note that the sharp peaks of the A15 phase in $(FD)_4$ at relatively high molecular weight ($4N$ = 347) stand in contrast to SAXS data collected on smaller, conformationally-asymmetric AB_n miktoarm stars with A = polylactide and B = poly(dodecyl acrylate) blocks,[52] where notable peak broadening is evident in AB_2 (N = 150) and AB_3 (N = 174) lacks a discernable A15 phase entirely. Figure 3c,d shows real-space depictions of the σ and A15 unit cells that were calculated from one-dimensional FDF SAXS patterns following an established procedure: fitting intensities with Le Bail refinement and charge flipping the resulting structure factor amplitudes to circumvent the crystallographic phase problem (see the Supporting Information for details).[62] The different micelles in each picture are false colored by Wyckoff position to accentuate their symmetry-(in)equivalent shapes and sizes.

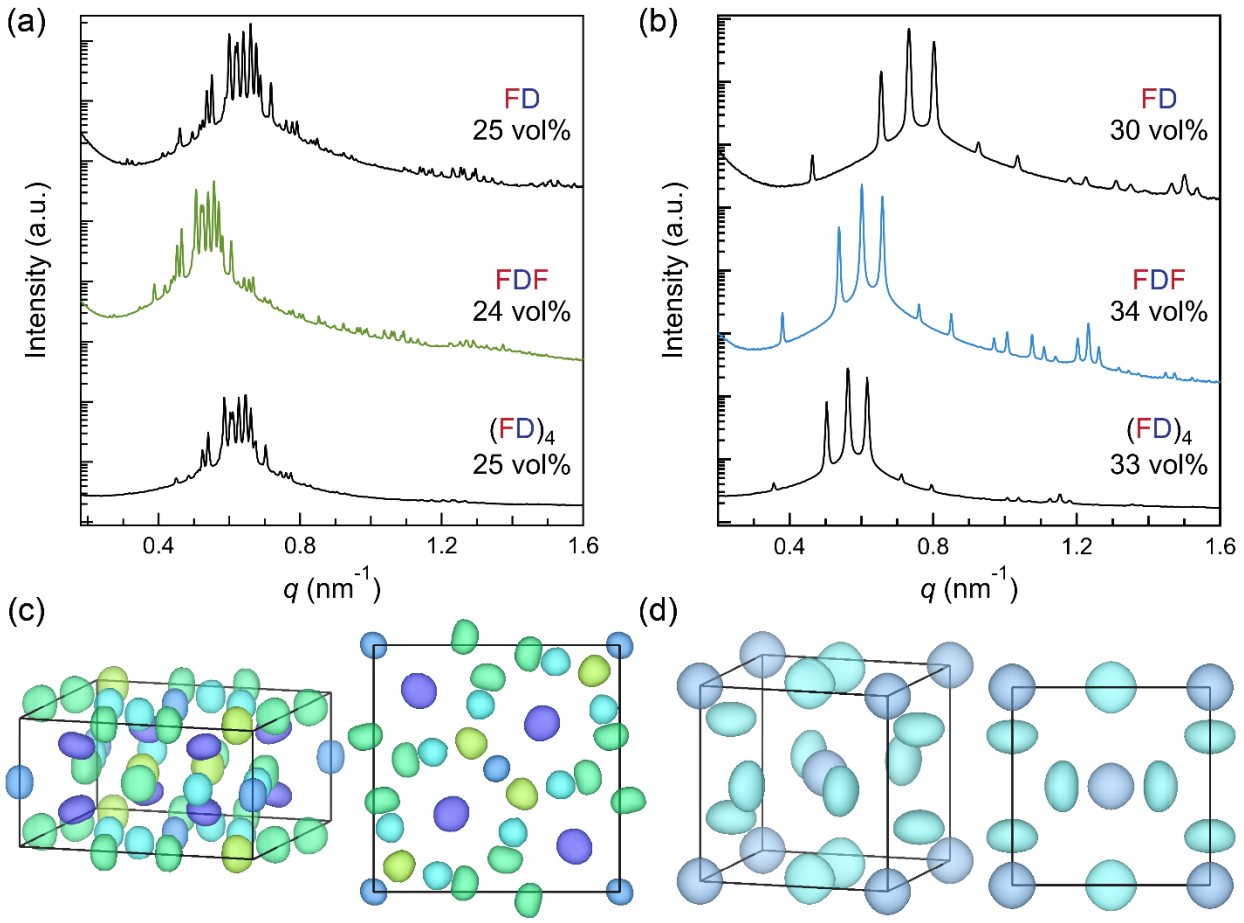

Figure 3. SAXS profiles of the (a) σ and (b) A15 phases in FD, FDF, and $(FD)_4$ block polymers obtained after isothermal annealing for ≥19 h at T = 25–120 °C. Unit cell electron density reconstructions (60% isosurface) of the (c) σ and (d) A15 phases generated from the highlighted FDF scattering traces; flat depictions are unit cell projections along the c-axis. False colors represent symmetry-distinct micelles occupying unique Wyckoff positions. The D block fills uncolored regions of each unit cell.

Following the discovery of σ and A15, the impact of conformational asymmetry on the phase behavior of each architecture was examined using SCFT simulations. Figure 4 presents the stable phase windows of AB diblocks, ABA triblocks, and $(AB)_4$ stars with the inclusion of TCP candidate phases, namely A15, C14, C15, and σ as a function of the statistical segment length ratio, ε, for fixed χN = 40. Similar architectural comparisons have been made previously under the

assumption of conformational symmetry ($\varepsilon = 1$)[16] or without considering TCP phases as possible stable structures,[18] meaning only the BCC and CPS sphere phases were included. Our phase diagrams demonstrate that conformational asymmetry ($\varepsilon > 1$) is predicted to stabilize the σ and A15 phases in ABA triblocks of length $2N$ and $(AB)_4$ stars of length $4N$, much like the analogous AB diblock copolymer melts with a degree of polymerization N. Although conformational asymmetry slightly shifts order–order phase boundaries in the ABA triblock and to a lesser extent the $(AB)_4$ stars relative to $\varepsilon = 1$, their mean-field phase behavior is for all practical purposes indistinguishable. While not explicitly simulated, we expect that this conclusion equally applies to $(AB)_3$ stars. We also note that the $(AB)_n$ architecture with B blocks connected at a star junction has some inherent architectural asymmetry which favors curvature toward the B domain — i.e., even in the absence of statistical segment length asymmetry it behaves as if $b_B > b_A$ — although this modest effect is not enough to support TCP phases.[16, 63] Evidently, with F and D blocks, $\varepsilon = b_A/b_B > 1$ is sufficient to overcome this architectural asymmetry and stabilize σ and A15.

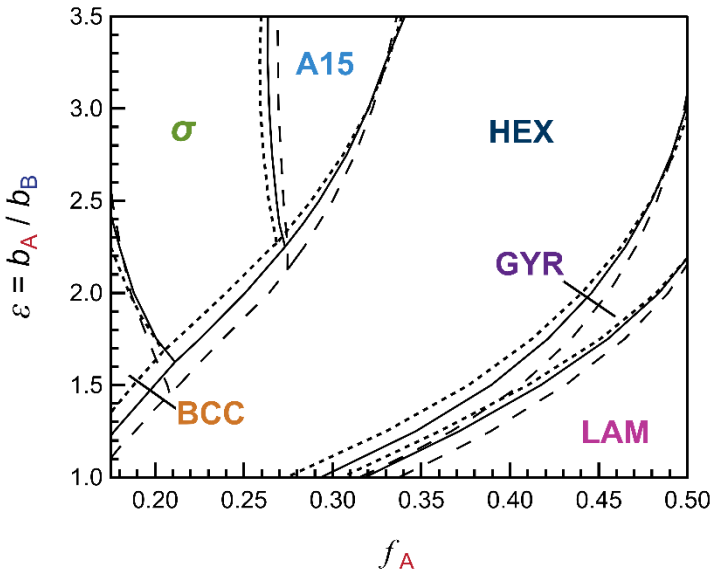

Figure 4. SCFT simulations that include TCP candidate phases (σ, A15, C14, and C15) predict the phase behavior of AB diblocks (dashed lines), ABA triblocks (black solid lines), and $(AB)_4$

stars (dotted lines) is almost indistinguishable for all values of conformational asymmetry (ε) at fixed $\chi N = 40$. Note that the $(AB)_4$ stars and ABA triblocks are four and two times larger (degrees of polymerization $4N$ and $2N$, respectively) than the AB diblocks (N) for comparison.[16]

Nominally equilibrium FD and FDF phase diagrams ($f_F \leq 0.50$) were constructed using variable-temperature synchrotron SAXS experiments complemented by dynamic mechanical thermal analysis to identify T_{ODT} values (Figure 5a,b, see Supporting Information for details). Both architectures self-assemble into BCC, σ, A15, HEX and GYR morphologies, however, the experimental self-assembly of FD and FDF shows striking differences. Pure A15 forms in multiple FDF samples across $f_F \approx 0.29$–0.35 versus at a single composition of FD ($f_F = 0.30$). Moreover, coexisting A15 and HEX phases were consistently identified in the diblock (Figure S16) and the fact that a small channel of pure A15 is found at even larger f_F is strange. Note that two other batches of FD prepared with $f_F \approx 0.27$ (not shown in Figure 5 for clarity, see Table S6) similarly formed mixed lattices. Repeated attempts to process these diblock and triblock samples by extended annealing or with various quench protocols did not resolve the unexpected differences nor the two-phase coexistence. At least three possible explanations could account for this unusual behavior. (1) Molar mass dispersity permits phase co-existence per the Gibbs phase rule, although we do not believe this effect dominates as $Đ < 1.13$ for all samples (Tables S2, S3, S6); if anything, the triblocks are slightly more disperse than the diblocks. (2) The influence of end-groups that are not accounted for in coarse-grained SCFT simulations may be non-negligible at low invariant degrees of polymerizations ($\overline{N}$, see Tables S2–S6). (3) Fluctuation effects, which also amplify at small $\overline{N}$, are known to play a role in the selection of TCP phases with diblock copolymers.[31] While fluctuation-corrected simulations analyzing TCP phase formation have not yet been performed on

symmetric triblocks, it is conceivable that architecture could tip the balance in favor of certain sphere phases which differ by miniscule amounts of intensive free energy.[31, 34]

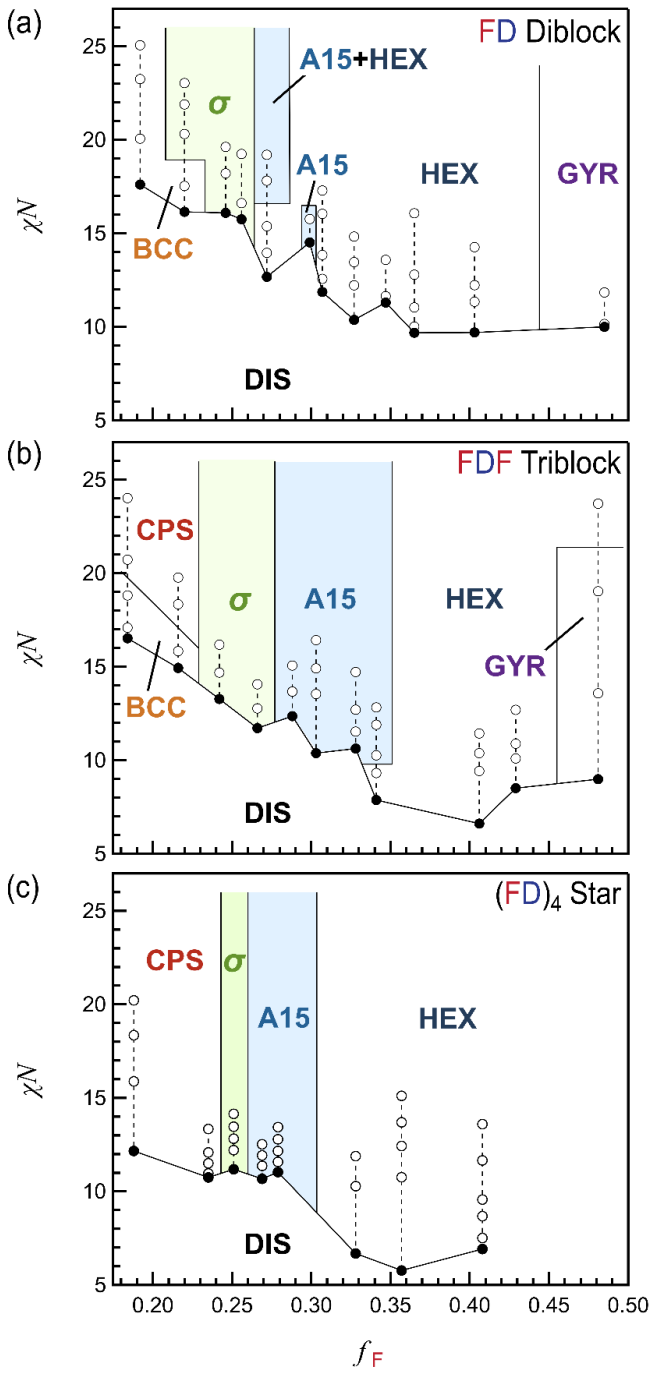

Figure 5. The experimental phase behavior of conformationally asymmetric (a) FD diblocks, (b) FDF triblocks, and (c) $(FD)_4$ radial stars is comparable but exhibits unexpected differences. Points

in phase space examined by SAXS are marked with open circles and $(\chi N)_{ODT}$ values identified using dynamic mechanical thermal analysis are indicated by filled circles. Data points obtained from each sample are connected with dashed lines. Interpolated phase boundaries (solid lines) are drawn at the compositional average of adjacent samples differing in morphology.

The phase diagrams of $(FD)_3$ and $(FD)_4$ radial stars resemble those of both the FD diblock and FDF triblock (Figures 5c and S17). As the number of arms increases, notable reductions in $(\chi N)_{ODT}$ are observed. This result is consistent with stars having greater configurational constraints that reduce the entropy of the disordered melt and therefore stabilize ordered phases to higher temperatures.[22] Overall, the star phase behavior qualitatively mirrors that of FDF triblocks, although the experimental lack of BCC order in lieu of CPS is surprising. While this result might also point to dispersity effects, we note that no two-phase windows were observed in the three or four-arm stars. Notably, the regions of σ and A15 stability in both $(FD)_3$ and $(FD)_4$ appear narrower than in FDF triblocks, consistent with SCFT predictions (Figure 4). As recently noted by Shi and coworkers,[42] the star architecture may regulate the bridging fraction of A segments across micelles, leading to a possible mechanism that controls the coordination number and biases formation of a particular lattice. Our results do not immediately support or refute this effect, but we have established the accessibility of TCP phases in architectures beyond linear diblocks, including ABA triblocks and $(AB)_n$ radial stars with conformationally-asymmetric A and B blocks ($b_A > b_B$).

Conformational asymmetry stabilizes interfacial curvature to larger f_A, resulting in the emergence of TCP sphere phases that adopt an optimal balance of particle sphericity and chain stretching.[43-44, 64] This expanded sphere-forming window is expected to follow an established sequence of CPS–BCC–σ–A15 as f_A increases.[31] Our SCFT simulations generally reflect this trend, as do the experimental phase diagrams, but significant quantitative discrepancies between

experiments and theory remain largely unresolved. Theoretically, the critical value of ε at which A15 first becomes stable depends slightly on architecture: $\varepsilon_{AB} \approx 2.13$, $\varepsilon_{ABA} \approx 2.25$, and $\varepsilon_{(AB)4} \approx 2.27$ (Figure 4). Each is significantly higher than our experimental estimate of $\varepsilon = 1.43$, even given the modest uncertainty associated with measuring F and D statistical segment lengths by rheology. While we cannot provide a conclusive explanation for this behavior, it may be related to the use of the idealized continuous Gaussian chain model in SCFT. The observed mismatch of experiment and SCFT is also consistent with other literature on low molecular weight block polymers involving different choices of A and/or B blocks.[31, 51] In general, theory overestimates the value of ε necessary to stabilize complex sphere phases at finite molecular weight, a condition also subject to fluctuations and dispersity. Here, the theoretical ε that is most consistent with experiments also depends on architecture. Whereas FD, $(FD)_3$, and $(FD)_4$ form A15 over a narrow range of compositions consistent with $\varepsilon_{theory} \gtrsim 2.13$, the wider window found in ABA triblocks ($f_F \approx 0.29 – 0.35$) more closely aligns with ε_{theory} circa 3.5. Nevertheless, F and D have enough conformational asymmetry from a mismatch in statistical segment lengths to stabilize both the σ and A15 phases, the details of which depend on molecular connectivity. We emphasize that this level of conformational asymmetry can be amplified further using the mikto architecture, which stabilizes TCP phases over an even wider range of volume fractions.[28, 52]

In summary, we have studied the complex phase behavior of AB, ABA, $(AB)_3$, and $(AB)_4$ linear and star block copolymers, where A = poly(trifluoroethyl acrylate) (F) and B = poly(dodecyl acrylate) (D). These materials are synthetically accessible via photo-mediated ATRP from various functional initiators, exhibit sizeable conformational asymmetry ($\varepsilon = 1.43$) due to the different statistical segment lengths of F and D, have a large interaction parameter ($\chi_{FD} = 84/T – 0.101$), and are thermally processable at convenient temperatures. Together, these attributes promote the

formation of TCP phases in all four architectures. Differences in the phase behavior of FD diblocks and FDF triblocks cannot be explained by mean-field SCFT simulations in contrast to conformationally-symmetric analogues, which suggests that our collective understanding of TCP phases at low degrees of polymerization remains incomplete. We anticipate that further studying the correlations between chemistry, molecular design, and self-assembly will provide useful insights in the quest to harness block copolymer phases and especially TCP morphologies in contemporary applications.

ASSOCIATED CONTENT

Supporting Information

Supporting Information is available free of charge on the ACS Publications website. Experimental methods, representative molecular characterization data (SEC, NMR, TGA, DSC), rheological evaluation of the entanglement molecular weight and an estimation of the statistical segment lengths of D and F homopolymers, representative SAXS characterization and indexed patterns, and a description of the electron density reconstruction methodology for the A15 and σ phases.

AUTHOR INFORMATION

Corresponding Authors

*Email: cbates@ucsb.edu (C.M.B)

*Email: hawker@mrl.ucsb.edu (C.J.H)

*Email: morganbates@ucsb.edu (M.W.B.)

Author Contributions

[#]S.M.B. and J.S. contributed equally. The manuscript was written by M.W.B. and C.M.B. Experiments were designed by S.M.B., J.S., C.Z., A.A., M.R., M.W.B., C.J.H., and C.M.B. and performed by S.M.B., J.S., C.Z., A.A., M.R., and M.W.B. Simulations were designed by J.L., D.C., K.T.D., and G.H.F and performed by J.L., D.C., and K.T.D. All authors have given approval to the final version of the manuscript.

Notes

The authors declare no competing financial interest.

Funding

The research reported here was supported by the National Science Foundation under Award No. DMR-1844987 (C.M.B.) and partially through the MRSEC Program under Award No. DMR-1720256 (IRG-2, G.H.F., C.J.H., C.M.B.). The research reported here made use of shared facilities of the UCSB MRSEC (NSF DMR-1720256), a member of the Materials Research Facilities Network (www.mrfn.org). Use was made of computational facilities purchased with funds from the National Science Foundation (CNS-1725797) and administered by the Center for Scientific Computing (CSC). The CSC is supported by the California NanoSystems Institute and the Materials Research Science and Engineering Center (MRSEC; NSF DMR-1720256) at UC Santa Barbara. S.M.B. and A.A. acknowledge the California NanoSystems Institute for an Elings Prize Fellowship in Experimental Science. A.A. is grateful to the European Union's Horizon 2020 research and innovation program for a Marie Curie Global Postdoctoral Fellowship. S.M.B. is grateful to the National Science and Engineering Research Council of Canada for the Banting Postdoctoral Fellowship. C.Z. acknowledges support from the Australian Research Council (CE140100036) and National Health and Medical Research Council for an Early Career Fellowship (APP1157440).

ACKNOWLEDGEMENTS

Portions of this work were performed at the DuPont-Northwestern-Dow Collaborative Access Team (DND-CAT) located at Sector 5 of the Advanced Photon Source (APS). DND-CAT is supported by Northwestern University, E.I. DuPont de Nemours & Co., and The Dow Chemical Company. This research used resources of the Advanced Photon Source, a U.S. Department of Energy (DOE) Office of Science User Facility operated for the DOE Office of Science by Argonne National Laboratory under Contract No. DE-AC02-06CH11357. Data were collected using an instrument funded by the National Science Foundation under Award Number 0960140. X-ray scattering experiments were also performed at the Stanford Synchrotron Radiation Lightsource, SLAC National Accelerator Laboratory, which is supported by the U.S. Department of Energy, Office of Science, Office of Basic Energy Sciences under Contract DE-AC02-76SF00515.

REFERENCES

1. Bates, C. M.; Bates, F. S., 50th Anniversary Perspective: Block Polymers—Pure Potential. *Macromolecules* **2017,** *50* (1), 3-22.
2. Sun, H.-J.; Zhang, S.; Percec, V., From structure to function via complex supramolecular dendrimer systems. *Chemical Society Reviews* **2015,** *44* (12), 3900-3923.
3. van ‘t Hag, L.; Gras, S. L.; Conn, C. E.; Drummond, C. J., Lyotropic liquid crystal engineering moving beyond binary compositional space – ordered nanostructured amphiphile self-assembly materials by design. *Chemical Society Reviews* **2017,** *46* (10), 2705-2731.
4. Zhang, W.-B.; Yu, X.; Wang, C.-L.; Sun, H.-J.; Hsieh, I. F.; Li, Y.; Dong, X.-H.; Yue, K.; Van Horn, R.; Cheng, S. Z. D., Molecular Nanoparticles Are Unique Elements for Macromolecular Science: From “Nanoatoms” to Giant Molecules. *Macromolecules* **2014,** *47* (4), 1221-1239.

5. Cabral, H.; Miyata, K.; Osada, K.; Kataoka, K., Block Copolymer Micelles in Nanomedicine Applications. *Chemical Reviews* **2018,** *118* (14), 6844-6892.
6. Bates, C. M.; Maher, M. J.; Janes, D. W.; Ellison, C. J.; Willson, C. G., Block Copolymer Lithography. *Macromolecules* **2014,** *47* (1), 2-12.
7. Luo, M.; Epps, T. H., Directed Block Copolymer Thin Film Self-Assembly: Emerging Trends in Nanopattern Fabrication. *Macromolecules* **2013,** *46* (19), 7567-7579.
8. Kennemur, J. G.; Yao, L.; Bates, F. S.; Hillmyer, M. A., Sub-5 nm Domains in Ordered Poly(cyclohexylethylene)-block-poly(methyl methacrylate) Block Polymers for Lithography. *Macromolecules* **2014,** *47* (4), 1411-1418.
9. Parkatzidis, K.; Wang, H. S.; Truong, N. P.; Anastasaki, A., Recent Developments and Future Challenges in Controlled Radical Polymerization: A 2020 Update. *Chem* **2020,** *6* (7), 1575-1588.
10. Zhang, Y.; Almodovar-Arbelo, N. E.; Weidman, J. L.; Corti, D. S.; Boudouris, B. W.; Phillip, W. A., Fit-for-purpose block polymer membranes molecularly engineered for water treatment. *npj Clean Water* **2018,** *1* (1), 2.
11. Bates, F. S.; Hillmyer, M. A.; Lodge, T. P.; Bates, C. M.; Delaney, K. T.; Fredrickson, G. H., Multiblock Polymers: Panacea or Pandora's Box? *Science* **2012,** *336* (6080), 434-440.
12. Bates, F. S.; Fredrickson, G. H., Block Copolymers---Designer Soft Materials. *Physics Today* **1999,** *52* (2), 32-38.
13. Huang, Y.-Y.; Hsu, J.-Y.; Chen, H.-L.; Hashimoto, T., Existence of fcc-Packed Spherical Micelles in Diblock Copolymer Melt. *Macromolecules* **2007,** *40* (3), 406-409.

14. Takenaka, M.; Wakada, T.; Akasaka, S.; Nishitsuji, S.; Saijo, K.; Shimizu, H.; Kim, M. I.; Hasegawa, H., Orthorhombic Fddd Network in Diblock Copolymer Melts. *Macromolecules* **2007,** *40* (13), 4399-4402.

15. Tyler, C. A.; Morse, D. C., Orthorhombic Fddd Network in Triblock and Diblock Copolymer Melts. *Physical Review Letters* **2005,** *94* (20), 208302.

16. Matsen, M. W., Effect of Architecture on the Phase Behavior of AB-Type Block Copolymer Melts. *Macromolecules* **2012,** *45* (4), 2161-2165.

17. Abetz, V.; Simon, P. F., Phase behaviour and morphologies of block copolymers. In *Block copolymers I*, Springer: pp 125-212.

18. Matsen, M. W.; Thompson, R. B., Equilibrium behavior of symmetric ABA triblock copolymer melts. *The Journal of Chemical Physics* **1999,** *111* (15), 7139-7146.

19. Mai, S.-M.; Mingvanish, W.; Turner, S. C.; Chaibundit, C.; Fairclough, J. P. A.; Heatley, F.; Matsen, M. W.; Ryan, A. J.; Booth, C., Microphase-Separation Behavior of Triblock Copolymer Melts. Comparison with Diblock Copolymer Melts. *Macromolecules* **2000,** *33* (14), 5124-5130.

20. Matsen, M. W.; Schick, M., Stable and Unstable Phases of a Linear Multiblock Copolymer Melt. *Macromolecules* **1994,** *27* (24), 7157-7163.

21. Wu, L.; Cochran, E. W.; Lodge, T. P.; Bates, F. S., Consequences of Block Number on the Order−Disorder Transition and Viscoelastic Properties of Linear $(AB)_n$ Multiblock Copolymers. *Macromolecules* **2004,** *37* (9), 3360-3368.

22. Olvera de la Cruz, M.; Sanchez, I. C., Theory of microphase separation in graft and star copolymers. *Macromolecules* **1986,** *19* (10), 2501-2508.

23. Herman, D. S.; Kinning, D. J.; Thomas, E. L.; Fetters, L. J., A compositional study of the morphology of 18-armed poly(styrene-isoprene) star block copolymers. *Macromolecules* **1987,** *20* (11), 2940-2942.

24. Matsen, M. W.; Schick, M., Microphase Separation in Starblock Copolymer Melts. *Macromolecules* **1994,** *27* (23), 6761-6767.

25. Jang, S.; Moon, H. C.; Kwak, J.; Bae, D.; Lee, Y.; Kim, J. K.; Lee, W. B., Phase Behavior of Star-Shaped Polystyrene-block-poly(methyl methacrylate) Copolymers. *Macromolecules* **2014,** *47* (15), 5295-5302.

26. Lee, C.; Gido, S. P.; Poulos, Y.; Hadjichristidis, N.; Tan, N. B.; Trevino, S. F.; Mays, J. W., π-Shaped double-graft copolymers: effect of molecular architecture on morphology. *Polymer* **1998,** *39* (19), 4631-4638.

27. Xenidou, M.; Beyer, F. L.; Hadjichristidis, N.; Gido, S. P.; Tan, N. B., Morphology of Model Graft Copolymers with Randomly Placed Trifunctional and Tetrafunctional Branch Points. *Macromolecules* **1998,** *31* (22), 7659-7667.

28. Grason, G. M.; Kamien, R. D., Interfaces in Diblocks: A Study of Miktoarm Star Copolymers. *Macromolecules* **2004,** *37* (19), 7371-7380.

29. Pochan, D. J.; Gido, S. P.; Pispas, S.; Mays, J. W.; Ryan, A. J.; Fairclough, J. P. A.; Hamley, I. W.; Terrill, N. J., Morphologies of Microphase-Separated A_2B Simple Graft Copolymers. *Macromolecules* **1996,** *29* (15), 5091-5098.

30. Lee, S.; Bluemle, M. J.; Bates, F. S., Discovery of a Frank-Kasper σ Phase in Sphere-Forming Block Copolymer Melts. *Science* **2010,** *330* (6002), 349-353.

31. Bates, M. W.; Lequieu, J.; Barbon, S. M.; Lewis, R. M.; Delaney, K. T.; Anastasaki, A.; Hawker, C. J.; Fredrickson, G. H.; Bates, C. M., Stability of the A15 phase in diblock

copolymer melts. *Proceedings of the National Academy of Sciences* **2019,** *116* (27), 13194-13199.

32. Frank, F. C.; Kasper, J. S., Complex alloy structures regarded as sphere packings. I. Definitions and basic principles. *Acta Crystallographica* **1958,** *11* (3), 184-190.
33. Frank, F. C.; Kasper, J. S., Complex alloy structures regarded as sphere packings. II. Analysis and classification of representative structures. *Acta Crystallographica* **1959,** *12* (7), 483-499.
34. Kim, K.; Schulze, M. W.; Arora, A.; Lewis, R. M.; Hillmyer, M. A.; Dorfman, K. D.; Bates, F. S., Thermal processing of diblock copolymer melts mimics metallurgy. *Science* **2017,** *356* (6337), 520-523.
35. Gillard, T. M.; Lee, S.; Bates, F. S., Dodecagonal quasicrystalline order in a diblock copolymer melt. *Proceedings of the National Academy of Sciences* **2016,** *113* (19), 5167-5172.
36. Natarajan, A. R.; Van der Ven, A., Connecting the Simpler Structures to Topologically Close-Packed Phases. *Physical Review Letters* **2018,** *121* (25), 255701.
37. Ungar, G.; Zeng, X., Frank-Kasper, quasicrystalline and related phases in liquid crystals. *Soft Matter* **2005,** *1* (2), 95-106.
38. Su, Z.; Hsu, C.-H.; Gong, Z.; Feng, X.; Huang, J.; Zhang, R.; Wang, Y.; Mao, J.; Wesdemiotis, C.; Li, T.; Seifert, S.; Zhang, W.; Aida, T.; Huang, M.; Cheng, S. Z. D., Identification of a Frank–Kasper Z phase from shape amphiphile self-assembly. *Nat. Chem.* **2019,** *11* (10), 899-905.
39. Baez-Cotto, C. M.; Mahanthappa, M. K., Micellar Mimicry of Intermetallic C14 and C15 Laves Phases by Aqueous Lyotropic Self-Assembly. *ACS Nano* **2018,** *12* (4), 3226-3234.

40. De Graef, M.; McHenry, M. E., *Structure of materials: an introduction to crystallography, diffraction and symmetry*. Cambridge University Press: 2012.

41. Xie, N.; Li, W.; Qiu, F.; Shi, A.-C., σ Phase Formed in Conformationally Asymmetric AB-Type Block Copolymers. *ACS Macro Letters* **2014,** *3* (9), 906-910.

42. Li, W.; Duan, C.; Shi, A.-C., Nonclassical Spherical Packing Phases Self-Assembled from AB-Type Block Copolymers. *ACS Macro Letters* **2017,** *6* (11), 1257-1262.

43. Grason, G. M.; DiDonna, B. A.; Kamien, R. D., Geometric Theory of Diblock Copolymer Phases. *Physical Review Letters* **2003,** *91* (5), 058304.

44. Reddy, A.; Buckley, M. B.; Arora, A.; Bates, F. S.; Dorfman, K. D.; Grason, G. M., Stable Frank–Kasper phases of self-assembled, soft matter spheres. *Proceedings of the National Academy of Sciences* **2018,** *115* (41), 10233-10238.

45. Grason, G. M. Frank Kasper Phases of Squishable Spheres and Optimal Cell Models *J. Club Condens. Matter Phys.*, 2016. https://doi.org/10.36471/jccm_january_2016_01.

46. Bates, F. S.; Fredrickson, G. H., Conformational Asymmetry and Polymer-Polymer Thermodynamics. *Macromolecules* **1994,** *27* (4), 1065-1067.

47. Milner, S. T., Chain Architecture and Asymmetry in Copolymer Microphases. *Macromolecules* **1994,** *27* (8), 2333-2335.

48. Qiang, Y.; Li, W.; Shi, A.-C., Stabilizing Phases of Block Copolymers with Gigantic Spheres via Designed Chain Architectures. *ACS Macro Letters* **2020,** *9* (5), 668-673.

49. Vavasour, J. D.; Whitmore, M. D., Self-consistent field theory of block copolymers with conformational asymmetry. *Macromolecules* **1993,** *26* (25), 7070-7075.

50. Matsen, M. W.; Schick, M., Microphases of a Diblock Copolymer with Conformational Asymmetry. *Macromolecules* **1994,** *27* (14), 4014-4015.

51. Schulze, M. W.; Lewis, R. M.; Lettow, J. H.; Hickey, R. J.; Gillard, T. M.; Hillmyer, M. A.; Bates, F. S., Conformational Asymmetry and Quasicrystal Approximants in Linear Diblock Copolymers. *Physical Review Letters* **2017,** *118* (20), 207801.

52. Bates, M. W.; Barbon, S. M.; Levi, A. E.; Lewis, R. M.; Beech, H. K.; Vonk, K. M.; Zhang, C.; Fredrickson, G. H.; Hawker, C. J.; Bates, C. M., Synthesis and Self-Assembly of AB_n Miktoarm Star Polymers. *ACS Macro Letters* **2020,** *9* (3), 396-403.

53. Sun, Y.; Tan, R.; Ma, Z.; Gan, Z.; Li, G.; Zhou, D.; Shao, Y.; Zhang, W.-B.; Zhang, R.; Dong, X.-H., Discrete Block Copolymers with Diverse Architectures: Resolving Complex Spherical Phases with One Monomer Resolution. *ACS Central Science* **2020,** *6* (8), 1386-1393.

54. Lewis, R. M.; Arora, A.; Beech, H. K.; Lee, B.; Lindsay, A. P.; Lodge, T. P.; Dorfman, K. D.; Bates, F. S., Role of Chain Length in the Formation of Frank-Kasper Phases in Diblock Copolymers. *Physical Review Letters* **2018,** *121* (20), 208002.

55. Barbon, S. M.; Rolland, M.; Anastasaki, A.; Truong, N. P.; Schulze, M. W.; Bates, C. M.; Hawker, C. J., Macrocyclic Side-Chain Monomers for Photoinduced ATRP: Synthesis and Properties versus Long-Chain Linear Isomers. *Macromolecules* **2018,** *51* (17), 6901-6910.

56. Discekici, E. H.; Anastasaki, A.; Kaminker, R.; Willenbacher, J.; Truong, N. P.; Fleischmann, C.; Oschmann, B.; Lunn, D. J.; Read de Alaniz, J.; Davis, T. P.; Bates, C. M.; Hawker, C. J., Light-Mediated Atom Transfer Radical Polymerization of Semi-Fluorinated (Meth)acrylates: Facile Access to Functional Materials. *Journal of the American Chemical Society* **2017,** *139* (16), 5939-5945.

57. Athina, A.; Bernd, O.; Johannes, W.; Anna, M.; Van Son, M. H. C.; Truong, N. P.; Schulze, M. W.; Discekici, E. H.; McGrath, A. J.; Davis, T. P.; Bates, C. M.; Hawker, C. J., One-Pot

Synthesis of ABCDE Multiblock Copolymers with Hydrophobic, Hydrophilic, and Semi-Fluorinated Segments. *Angewandte Chemie International Edition* **2017,** *56* (46), 14483-14487.

58. Hiemenz, P. C.; Lodge, T. P., *Polymer chemistry*. CRC press: 2007.
59. Fetters, L. J.; Lohse, D. J.; Richter, D.; Witten, T. A.; Zirkel, A., Connection between Polymer Molecular Weight, Density, Chain Dimensions, and Melt Viscoelastic Properties. *Macromolecules* **1994,** *27* (17), 4639-4647.
60. Fetters, L. J.; Lohse, D. J.; Graessley, W. W., Chain dimensions and entanglement spacings in dense macromolecular systems. *Journal of Polymer Science Part B: Polymer Physics* **1999,** *37* (10), 1023-1033.
61. Hahn, T.; Shmueli, U.; Arthur, J. W., *International tables for crystallography*. Reidel Dordrecht: 1983; Vol. 1.
62. Palatinus, L.; Chapuis, G., SUPERFLIP - a computer program for the solution of crystal structures by charge flipping in arbitrary dimensions. *Journal of Applied Crystallography* **2007,** *40* (4), 786-790.
63. Chen, L.; Qiang, Y.; Li, W., Tuning Arm Architecture Leads to Unusual Phase Behaviors in a $(BAB)_5$ Star Copolymer Melt. *Macromolecules* **2018,** *51* (23), 9890-9900.
64. Lee, S.; Leighton, C.; Bates, F. S., Sphericity and symmetry breaking in the formation of Frank–Kasper phases from one component materials. *Proceedings of the National Academy of Sciences* **2014,** *111* (50), 17723-17731.

FOR TABLE OF CONTENTS USE ONLY

Architecture Effects in Complex Spherical Assemblies of $(AB)_n$-type Block Copolymers

Stephanie M. Barbon, Jung-Ah Song, Duyu Chen, Cheng Zhang, Joshua Lequieu, Kris T. Delaney, Athina Anastasaki, Manon Rolland, Glenn H. Fredrickson, Morgan W. Bates, Craig J. Hawker, and Christopher M. Bates